Coupling of multi-LO phonons to crystal-field excitations in UO_2 studied by Raman spectroscopy

2008 J. Phys.: Condens. Matter 20 085202

(http://iopscience.iop.org/0953-8984/20/8/085202)

J. Phys.: Condens. Matter **20** (2008) 085202 (8pp) doi:10.1088/0953-8984/20/8/085202

Coupling of multi-LO phonons to crystal-field excitations in UO_2 studied by Raman spectroscopy

Tsachi Livneh

Department of Physics, Nuclear Research Center, Negev, PO Box 9001, Beer-Sheva 84190, Israel

E-mail: T.Livneh@nrcn.org.il

Received 26 September 2007
Published 1 February 2008
Online at stacks.iop.org/JPhysCM/20/085202

Abstract

Electronic Raman spectra of UO_2 were measured under high hydrostatic pressure up to 21.5 GPa at room temperature. Resonant coupling was found between four (instead of the expected two) $^3H'_4 \rightarrow {}^3F'_2$ intermultiplet crystal-field (CF) excitations (γ_1–γ_4 ranges from 4130 to 4580 cm^{-1}) and nLO phonons ($n = 1$–4, $\omega_{LO} \approx 578$ cm^{-1}). The additional two CF excitations concurrently emerge under high pressure and are characterized by significantly higher pressure coefficients. An increase in pressure and excitation energy beyond the onset of absorption at ~2 eV enhances the resonant coupling, similar to that previously found for multi-LO phonon Raman scattering. The pressure coefficients of the CF–multi-LO coupled mode frequencies fit well with the sum of the pressure coefficients of their CF and nLO constituents. The very good correlation between the positions of the CF + nLO Raman bands and previously measured optical absorption bands points to the significant contribution of LO phonon-assisted CF electronic transitions to the absorption spectrum. These findings are attributed to the strong interactions between electrons and LO phonons, which play an important role in the electronic properties of UO_2.

(Some figures in this article are in colour only in the electronic version)

1. Introduction

It is well known that the greater spatial extent of the 5f electrons of the actinide ions relative to the 4f electrons of the lanthanide ions leads to a stronger crystal-field (CF) potential [1, 2]. In UO_2 the large CF interactions lead to substantial mixing of 5f states with different J. In a cubic coordination the nine-fold degeneracy of the $J = 4$ ground state is partially removed. Rahman and Runciman (RR) [3] were the first to calculate the parameters which enter the CF Hamiltonian. Later, inelastic neutron scattering (INS) measurements [4–7] showed that the RR calculation overestimated both the J mixing and the CF excitation energies. Calculations of the corrected CF parameters estimated the two higher CF levels of the $^3F'_2$ first excited multiplet [6, 7] and the four levels of the $^3H'_5$ second excited state [7].

Optical spectroscopy was shown to be instructive in revealing the role played by the $5f^2$ band [1]: after the corrected CF parameters were introduced, the complex absorption spectra were reassigned [8]. However, some discrepancies still exist between the experimental absorption band energies [1, 8, 9] and the calculated ones [8]. Furthermore, many of the absorption bands are as yet unassigned. The difficulty in reliably assigning electronic transitions in UO_2 is mainly attributed [7] to the CF potential, being comparable in magnitude to the spin–orbit coupling, as well as the tendency of electronic transitions to couple to phonons. Those significantly complicate the spectra.

In addition to absorption and reflectivity measurements, the energy levels of the lower multiplet $^3F'_2$ and $^3H'_5$ terms are potentially accessible by means of INS and electronic Raman (ER) spectroscopy. A high energy transfer (HET) spectrometer was shown to be useful in detecting intermultiplet excitations with energies up to ~1 eV in various systems [7], but not in UO_2 [6]. As to ER spectroscopy, since the Stokes scattering intensity is proportional to $(E_i–E_{CF})^4$ (E_i and E_{CF} are the excitation and CF energies, respectively) for a suitable E_i high

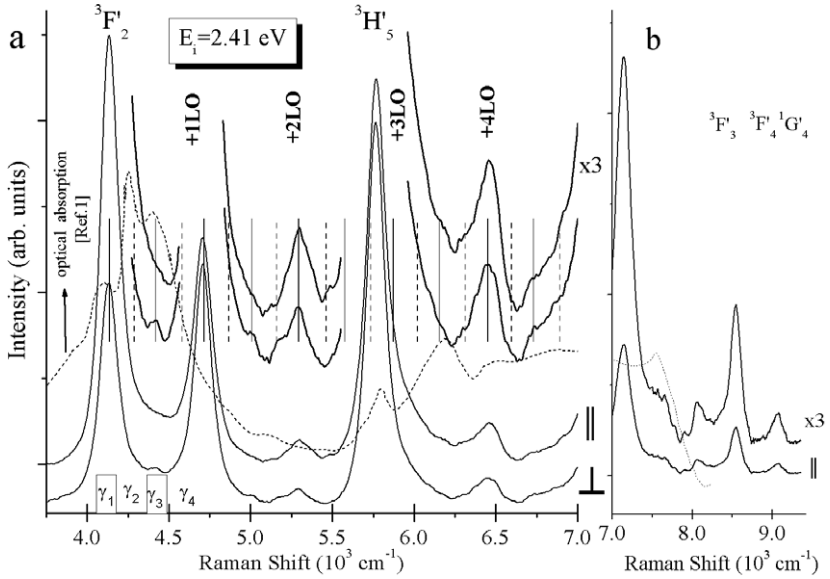

Figure 1. (a) Electronic–phononic Raman spectra in UO_2 with $E_i = 2.41$ eV, over the range of 3800–7000 cm^{-1} (solid line) with $\vec{\mathbf{E}}$i ∥ $\vec{\mathbf{E}}$s and $\vec{\mathbf{E}}$i ⊥ $\vec{\mathbf{E}}$s polarization configurations. The dashed line is for the room temperature absorption spectrum of UO_2 measured by Schoenes [1]. The positions of γ_1^n and γ_3^n ($n = 0$–4) are indicated with solid black and gray lines, respectively, and γ_2^n and γ_4^n with dashed black and gray lines, respectively. (b) Electronic–phononic Raman spectra over the range of 7000–9300 cm^{-1}. Some parts of the spectra are three-fold magnified for clarity.

enough to increase the scattering cross section, but limited by the absorptivity of UO_2 [1, 9], the $^3F'_2$ and $^5H'_3$ terms should be accessible. However, no assignment of intermultiplet electronic Raman scattering has yet been published for UO_2, or for other 5f electron systems.

In a recent study of the phononic Raman scattering in UO_2, up to sixth-order multi longitudinal optical (LO) phonon bands were detected. The Raman scattering intensity has been shown to follow the UO_2 absorption profile [10] with a threshold of ∼2.0 eV [1, 9]. This result was attributed to the existence of strong interactions between electrons and LO phonons, which is known to play an important role in the electronic properties of UO_2 [11, 12].

The strength of electron–phonon interactions, which is manifested by the high intensities of the LO band and its first overtone, is 'tuned' by the application of high pressure [10]. A pressure-induced resonance red-shift is consistent with pressure-dependent optical reflectivity measurements [13], which showed a ∼300 cm^{-1} GPa^{-1} shift in the position of the reflectivity edge. Furthermore, above ∼15 GPa a number of narrow optical transitions were observed in the reflectivity spectrum and have been attributed to transitions within the $5f^2$ multiplet. It has been suggested that the increasing strength of these, normally dipole-forbidden excitations, indicates an increasing admixture of presumably d-like character to the $5f^2$ configuration.

In this paper we investigate the UO_2 room temperature pressure-dependent intermultiplet electronic Raman scattering up to ∼1 eV and demonstrate the resonant coupling between LO phonons and U^{4+} CF excitations. As for multi-phonon scattering [10], the resonance conditions are shown to be sensitive to excitation energy E_i, as well as to pressure. By correlating the ER band positions with that of the absorption spectrum [1, 9] we show that the latter is strongly affected by the coupling of CF excitations with LO phonons.

2. Experimental details

A UO_2 pellet was synthesized by sintering of UO_2 powder in a hydrogen flow at 1700 °C. Electrochemical polishing of the pellet was followed by XRD measurements in order to verify the structural quality of the sample. The pellet was constructed from ∼20 μm single crystals with various unidentified crystallographic orientations. Backscattering geometry Raman measurements were obtained from a Renishaw dispersive spectrometer, using an objective of 50× (NA = 0.8) at two excitation energies of 1.96 and 2.41 eV. In the pressure-dependent measurements a 30 μm grain was inserted in a Tel-Aviv type diamond anvil cell [14] with solid Ar, serving as a pressure transmitting medium. Pressure dependent Raman measurements were done by using a ×40 long focal length objective. Pressure was measured by the Ruby luminescence method [15].

3. Results and discussions

3.1. Raman scattering under ambient pressure

In what follows we describe the measured electronic Raman spectrum of UO_2 over the 3800–9300cm^{-1} range, assign the spectrum according to the calculated intermultiplet CF transitions [8], which are shown in table 1, and compare our results with optical absorption spectroscopy, measured at two different laboratories [1, 9]. Some remarkable correlations have been revealed between the ER and absorption, which points to the crucial role in both spectra of the coupling

Table 1. The correlation between Raman scattering and absorption [9] band positions for various CF splittings, with the indicated prominent eigenvector component(s) [8]. The expected band positions that agree with the proposed assignments are also shown. $\Delta \approx 150\ \mathrm{cm}^{-1}$ and $\omega_{\mathrm{LO}} \approx 578\ \mathrm{cm}^{-1}$ [1].

Prominent eigenvector component(s) [8]	Calculated energy (cm^{-1}) [8]	Absorption band position (cm^{-1}) [9]	Assignment	Raman band position (cm^{-1})	Expected Raman band position (cm^{-1})
$^3F_2(\Gamma_5)$	4010	4220	γ_1	4130	
			$\gamma_2 = \gamma_1 + \Delta$	4280[a]	
$^3F_2(\Gamma_3)$	4430	4400	γ_3	4420	
			$\gamma_4 = \gamma_3 + \Delta$	4580[a]	
		4720	γ_{1+}LO	4712	4708
			γ_{2+}LO	(?)	4858
		4960	γ_{3+}LO	5005	4998
		5150	γ_{4+}LO	5160	5158
		5280	γ_{1+}2LO	5292	5286
		5440	γ_{2+}2LO	5470	5436
		5610	γ_{3+}2LO	(?)	5576
			γ_{4+}2LO	(?)	5736
$^3H_5(\Gamma_4)$	5730	5780	δ_1	5768	
			γ_{1+}3LO	∼5870	5864
		6000	γ_{2+}3LO	6020	6014
			γ_{3+}3LO	6150	6154
$^3H_5(\Gamma_3)$	6040	6150	δ_2		
			γ_{4+}3LO	6320	6314
			γ_{1+}4LO	6450	6442
$^3H_5(\Gamma_4)$	6470	6460	δ_3		
			γ_{2+}4LO	6600	6592
		6740	δ_{2+}LO?		
			γ_{3+}4LO	6725	6732
			γ_{4+}4LO	6905	6892
$^3H_5$, $^3F_3(\Gamma_5)$	6990	7000	δ_4		
				7149	
		7560	δ_{4+}LO?	7561	
		7940			
$^3F_3(\Gamma_2)$	8050	8090	ε_1	8060	
$^3F_4$, $^1G_4(\Gamma_4)$	8190	8260	ε_2		
$^3F_3(\Gamma_5)$	8460	8470			
		8520	ε_3	8549	
$^1G_4$, $^3H_6$, $^3F_4$, $^3F_3$, $^3H_5(\Gamma_4)$	8770	8800	ε_4		
$^3F_4$, $^1G_4$, $^3H_6$, $^3H_4(\Gamma_3)$	8970	8980	ε_5	9070	

[a] Not observed under ambient pressure.

between CF and LO phonons and to UO_2 being a system of strong interacting electrons and phonons [11, 12].

Figure 1(a) shows the electronic–phononic Raman spectra in UO_2 over the range of 3800–7000 cm^{-1} with an excitation energy of $E_{\mathrm{i}} = 2.41$ eV (solid line) compared with the room temperature absorption spectrum of UO_2 measured by Schoenes [1] (dashed line). In order to distinguish the weak spectral features both $\vec{\mathbf{E}}\mathrm{i} \parallel \vec{\mathbf{E}}\mathrm{s}$ and $\vec{\mathbf{E}}\mathrm{i} \perp \vec{\mathbf{E}}\mathrm{s}$ polarization configurations are shown. Figure 1(b) shows the electronic–phononic Raman spectra over the range of 7000–9300 cm^{-1}. $^3F_2$ is the predominant component of the first excited multiplet, denoted as $^3F_2'$, and is split into a Γ_5 triplet (4130 cm^{-1}) and a Γ_3 doublet (4420 cm^{-1}). However, detailed analysis of the ER spectra reveals a sequence of $E_{\mathrm{CF}} + n\mathrm{LO}$ ($n = 1$–4)[1]. This is not only the case for the $^3F_2'$ (Γ_5) and $^3F_2'$ (Γ_3) splittings, denoted by γ_1 and γ_3, respectively, but also for bands positioned at $^3F_2'(\Gamma_5) + \Delta$ and $^3F_2'(\Gamma_3) + \Delta$ ($\Delta \approx 150\ \mathrm{cm}^{-1}$). The latter are denoted by γ_2 and γ_4, respectively. The formation of the triplet sequence of bands had previously been detected in the absorption spectrum [1] and had been assigned to the emission and absorption of a ∼160 cm^{-1} phonon from an unassigned electronic transition at ∼4240 cm^{-1}. We shall discuss below a different assignment.

In figure 2 the positions of $\gamma_m + n\mathrm{LO}$ electronic–phononic sequences (denoted as γ_m^n with $\gamma_m^0 \equiv \gamma_m$) are plotted as a function of n for $m = 1$–4 and $n = 0$–4. The values of ω_{LO}, which are extracted from the linear fits of γ_1^n (n) and γ_3^n (n) (solid lines), are in very good agreement with the literature value of $\omega_{\mathrm{LO}} = 578\ \mathrm{cm}^{-1}$ [1]. Linear fits for γ_2^n (n) and γ_4^n (n) are also shown by dashed lines. Their ambient pressure values could only be extrapolated from the fits, since, unlike the former two bands, γ_2 and γ_4 CF transitions emerge only under high hydrostatic pressure (see below). By using $\omega_{\mathrm{LO}} = 578\ \mathrm{cm}^{-1}$, γ_2 and γ_4 are found at 4285 cm^{-1} and 4585 cm^{-1}, respectively, and are denoted in figure 2 with empty symbols.

Figure 3 shows the fourth derivative spectra of the optical absorption over the range of 4700–5700 cm^{-1} taken from Griffiths and Hubbard [9], which enabled the resolution of some 'hidden' weak bands in the absorption spectrum.

[1] The $\gamma_1 + 3\mathrm{LO}(\gamma_1^3)$ band appears as a 'hidden' shoulder at ∼5870 cm^{-1} to the δ_1 band. This assignment is supported by the higher intensity for $E_{\mathrm{i}} = 2.41$ eV relative to 1.96 eV.

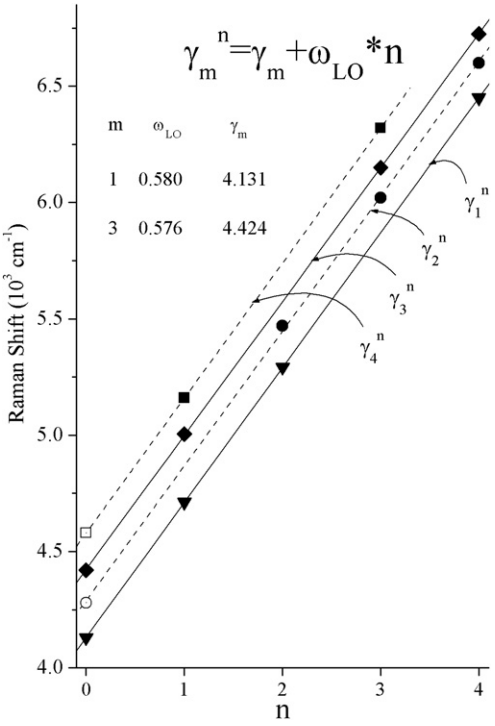

Figure 2. The positions of the various electronic–phononic sequences $\gamma_m^n(\gamma_m + n\text{LO})$ with $m = 1$–4 and $n = 0$–4, as a function of n. $\omega_{\text{LO}} = 578 \pm 2$ cm^{-1} is extracted from the linear fits of $\gamma_1^n(n)$ and $\gamma_3^n(n)$ (solid lines). In dashed lines linear fits for $\gamma_2^n(n)$ and $\gamma_4^n(n)$ are also shown. γ_2 and γ_4, found at 4285 cm^{-1} and 4585 cm^{-1}, respectively, are denoted with empty symbols.

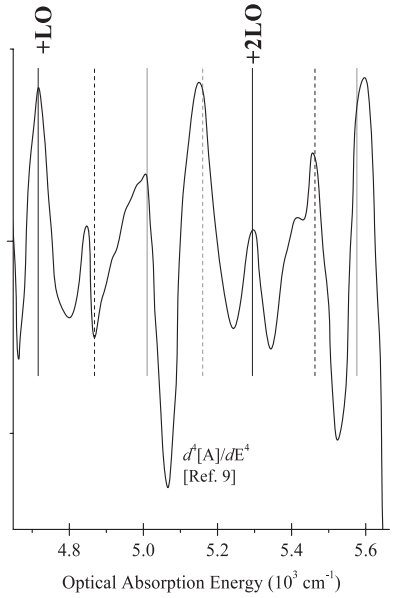

Figure 3. The optimized fourth derivative optical absorption spectrum of UO_2 over the range of 4700–5700 cm^{-1} measured by Griffiths and Hubbard [9], compared with the calculated 'expected' positions of $\gamma_1^1 - \gamma_3^2$.

Since over this energy range no pure CF excitations are expected [7, 8], all bands in that spectral region should exclusively be attributed to electronic–phononic coupled modes. Focusing on that spectral region should therefore serve as a test for their appearance in the absorption spectra. Remarkably, the same transitions appear in both Raman scattering and absorption spectra. This correlation clarifies the origin of some of the as yet unassigned features in the absorption spectra [9] and supports the interpretation of the Raman spectra in figure 1(a).

When the coupling between extended phonons and localized CF excitation is strong, the electronic and phonon modes are mixed in the region where the dispersion curves cross [2, 16]. Coupled CF-phonon modes are expected if the CF excitation has energy close to that of a phonon of the same symmetry and the coupling constant is large compared to the width of the phonon dispersion.

Mixtures of excitations due to strong coupling have been previously found in various systems: (i) intermetallic compounds like $CeAl_2$, where CF excitation and low lying vibrational modes of the Ce sublattice are involved in 'bond state' formation [17–19]; (ii) high T_c superconductors like rare earth (RE) cuprates ($REBa_2Cu_3O_x$, $6 \leqslant x \leqslant 7$) [16], where the CF excitations are coupled to oxygen phonons. Pressure-induced shifts which are different for the two manifolds have also been used to explore these systems [20].

Unlike the case of the above mentioned mixed electronic–phononic modes, the coupled CF + nLO modes in the case of UO_2 are not mixed modes since $E_{\text{CF}} \approx 8E_{\text{LO}}$ (E_{LO} being the LO phonon energy). Those are a manifestation of the strong electron–phonon coupling in UO_2 [11, 12]. The mechanism of polaron formation is known to enhance phonon-assisted optical transitions with a transition probability related to the distribution of the LO phonons [12]. This electronic–phononic coupling is clearly observed in the electronic Raman spectrum, which is shown in this study, as well as in optical absorption measurements conducted by others [1, 9] (see figure 1(a)). To our knowledge, such a phenomenon has not yet been found for other studied systems.

Due to the large number of bands and to the complexity of the various assignments, it is not always possible to separate the pure CF bands from the CF + nLO bands, particularly for the $\delta_1 - \delta_4$ $^3H_5'$ CF splittings. Despite their strong and distinct appearance in the absorption spectrum, which supports their assignment as pure CF bands, pressure-dependent data to be shown below strongly suggest that only δ_1 among the four $^3H_5'$ bands has significant intensity in the ER spectrum. For example, a band at ~6460 cm^{-1} can be assigned either to the γ_1^4 band or to the $^3H_5'(\Gamma_{4b})$ CF δ_2 band, or to both (see table 1). The formation of a *complete set* of $\gamma_m, m = 1$–4 bands with $n = 0$–4 strongly indicates that the former dominates the signal.

Finally, as a result of the significant spectral overlap between the majority of the δ_m^n and the γ_m^n bands, we cannot conclusively argue in favor of the detection of δ_m^n bands in the absorption, as well as in the ER spectra. This is unlike the case of the γ_m^n bands. More precise *ab initio* calculations are needed to unambiguously specify the positions of δ_1–δ_4 as well as the higher CF excitations, in order to conclude for which CF excitations the multi-LO phononic coupling scheme applies.

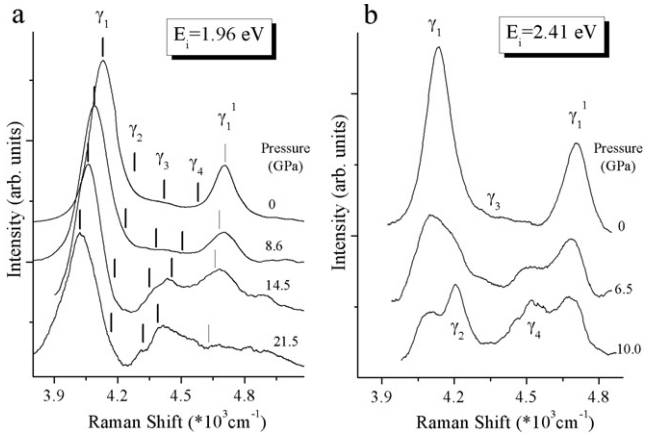

Figure 4. (a) The UO_2 Raman spectra (after applying a smoothing procedure) with $E_i = 1.96$ eV under the indicated high pressures over the range of 0–21.5 GPa. The expected values of $\gamma_1 - \gamma_4$ and of γ_1^1, which have been calculated by using equation (1), are also marked. (b) The UO_2 Raman spectra (after applying a smoothing procedure) with $E_i = 2.41$ eV under the indicated high pressures over the range of 0–10 GPa (see footnote 2).

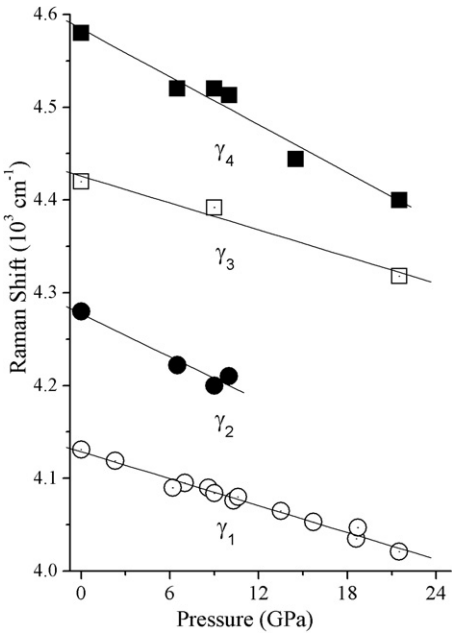

Figure 5. (a) Linear fits of the pressure-dependent $\gamma_1 - \gamma_4$ peak positions. The ambient pressure band positions for γ_2 and γ_4 are extrapolated from figure 2.

3.2. Raman scattering under high pressure

The application of high pressure to UO_2 changes the local field around the U^{4+} ion and provides a mean to continuously 'tune' the energies of the various CF excitations among the $5f^2$ electronic states. Since the pressure that is applied in our study (<22 GPa) is not sufficient to induce the known CaF_2-type → $PbCl_2$-type structural phase transition [21], the pressure will only vary the inter-atomic distances while the symmetry around the U^{4+} ion is not expected to be modified significantly.

In a previous study of the effect of pressure on the resonant multi-phonon Raman scattering in UO_2 [10], three main factors were found for the pressure-dependent behavior of the 1LO and 2LO bands: (i) a red-shift in the onset of resonance, which is related to the decrease in the band gap energy; (ii) an increase in the relative intensities of the bands, due to the increase in electron–phonon interactions; (iii) decrease in the penetration depth of the incident and scattered light, due to the increased absorption. An interplay between the first two factors (increasing) and the third (decreasing) was found to dictate the intensity of the LO band and its first overtone.

3.2.1. The $\gamma(^3H_4' \rightarrow {}^3F_2')$ excitations. The resonant coupling between multi-LO phonons and localized U^{4+} intermultiplet $^3H_4' \rightarrow {}^3F_2'$ CF excitations is evident from the increase in the intensity ratios of the CF + nLO bands relative to that of the pure CF excitations, $I\gamma_1^1/I\gamma_1$ and $I\gamma_1^2/I\gamma_1$. The latter is a factor of ∼1.5 and ∼3, for $E_i = 1.96$ eV and 2.41 eV, respectively. The question arises of whether some of the coupled modes, which are not detected for $E_i = 1.96$ eV under ambient conditions, will appear as a result of red-shifting the resonance onset with increasing pressure.

Figure 4(a) shows the Raman spectra taken for varying pressures in the range of 0–21.5 GPa with $E_i = 1.96$ eV, while figure 4(b) depicts Raman spectra at varying pressures over the range of 0–10 GPa with $E_i = 2.41$ eV.[2] Pressure coefficients of the four γ bands were derived in figure 5. From a linear fit of the pressure-dependent γ_1 peak, a pressure coefficient $(\partial\omega\gamma_1/\partial P) = -4.8 \pm 0.4$ cm^{-1} GPa^{-1} is extracted. Pressure coefficients ∼−7.8, ∼−4.8, ∼−8.6 of the peaks of the $\gamma_2 - \gamma_4$ bands are also obtained, although, in general, they are acquired with less confidence than for γ_1.[3] γ_1 and γ_3 have apparently similar pressure coefficients, and so do γ_2 and γ_4. However, the coefficients for the latter pair are significantly higher than for the former one.

The pressure-induced red-shift of the CF excitations is presumably related to the spatial expansion of the f orbitals of U^{4+}, which cause an increase in the covalency of the U–O bond (Nephelauxetic model). This effect has been suggested to play a significant role in explaining the CF transition pressure-induced red-shift in lanthanides 4f systems of Pr^{+3} in $LaCl_3$ [22] and Eu^{+3} in lithium borate glass [23].

We look into the pressure coefficients of the various coupled CF–multi-LO bands by combining the measured pressure coefficient of the γ_m peaks with that of the LO mode, $(\partial\omega_{LO}/\partial P) = 1.45 \pm 0.04$ cm^{-1} GPa^{-1} [10]. In this way the pressure coefficient of the coupled mode frequencies is the sum of the pressure coefficients of their CF and nLO constituents. We therefore calculate the 'expected' position of each of the γ_m^n according to:

$$\omega_{\gamma_m^n}(P) = \omega_{\gamma_m^n}(0) + ((\partial\omega_{\gamma m}/\partial P) + n \cdot (\partial\omega_{LO}/\partial P)) \cdot \Delta P, \quad n = 0\text{–}4. \tag{1}$$

[2] For $E_i = 2.41$ eV long measurement times are required due to the penetration depth being steeply decreasing with increasing pressure. Consequently, we are limited to pressures of about 10 GPa.

[3] The smaller separation between the various γ bands (∼150 cm^{-1}) relative to the sum of their half widths (∼200 cm^{-1}) imposes some difficulties on their assignment. The emergence of a sub-band structure under high pressure further complicates the task.

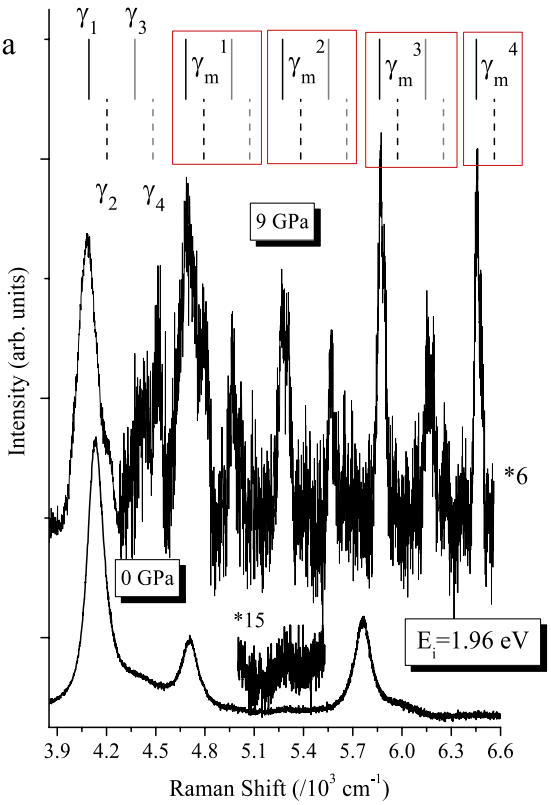

Figure 6. The complete sequence of γ_m^n, $m = 1$–4, $n = 0$–4 bands (top spectrum), which is activated by the application of 9 GPa pressure. The spectrum above 4300 cm^{-1} is magnified six-fold. Note that at ambient pressure (bottom spectrum) the CF–multi-LO phonon bands with $n > 1$ are barely detected. The calculated $\gamma_1^n - \gamma_4^n$ 'expected' band positions (according to equation (1)) are framed for each n. γ_1^n and γ_3^n are indicated with solid black and gray lines, respectively, and for γ_2^n and γ_4^n with dashed black and gray lines, respectively.

The expected values of $\gamma_1 - \gamma_4$ and of γ_1^1, which have been calculated by using equation (1), are also marked in figure 4(a). It is clear that the γ_2 and γ_4 bands, which are practically invisible under ambient conditions, emerge concurrently under pressure as their intensity increases relative to that of the γ_1 band. It is noteworthy that the $I\gamma_4/I\gamma_1$ pressure dependence for $E_i = 2.41$ eV is about an order of magnitude steeper than for $E_i = 1.96$ eV. This difference is attributed to the different positions of the two E_i relative to the absorption onset.

Figure 6 shows the *complete sequence* of γ_m^n, $m = 1$–4, $n = 0$–4 bands for $E_i = 1.96$ eV, which is activated by application of 9 GPa pressure (top spectrum). At ambient pressure (bottom spectrum) the higher CF–multi-LO phonon bands are barely detected; they diminish as E_i decreases from 2.41 eV (see figure 1(a)) towards the absorption edge energy of ∼2 eV. Related behavior was found for LO multi phonon bands, where it indicated the resonant nature of the scattering process [10]. Similarity between the two manifolds is also found when pressure is increased: the increase in electronic–phononic coupling is evidenced from the enhancement of γ_m^n, $m = 1$–4, $n = 2$–4, for the 9 GPa spectra relative to that of zero pressure. Weak coupled bands with *emission* of LO phonons (i.e. CF + nLO bands with $n = -1, -2$) have also been detected (not shown).

In figure 7(a) the top spectrum shown in figure 6 is 'sliced' into segments that are shifted by $-n\omega_{LO}$ (9 GPa). In figure 7(b) we fit the central band positions for $m = 1$, 3 and $n = 0$–4 to the linear equation $\gamma_m^n(P) = \gamma_m(P) + \omega_{LO}(P) \cdot n$. The extracted LO frequency is very close to the expected value of ω_{LO} (9 GPa) and a value for $\gamma_3 = 4371$ cm^{-1}, although difficult to distinguish in the spectrum, is consistent with the expected value of $(\partial\omega_{\gamma 3}/\partial P) \approx -4.8$, which has been obtained from figure 5.

In the electronic Raman spectrum of UO_2 four ($\gamma_1 - \gamma_4$) $^3H_4' \rightarrow {}^3F'_2$ intermultiplet CF excitations are detected, rather than the two expected according to the accepted CF scheme analysis [3]. It is suggested that the detection of the 'extra' two bands is due to the splitting of the $^3H_4'(\Gamma_5)$ CF ground state as a result of the deviation from cubic symmetry around the U^{4+} ion. Moreover, looking closer into the structure of some of the γ bands upon the application of high pressure it is evident that those split into up to seven to eight sub-bands, which are separated by intervals of 20–40 cm^{-1}. The effect is shown in the inset of figure 7(a), which presents the $\gamma_1 - \gamma_2$ spectral region at 10 GPa and $E_i = 1.96$ eV. Also here the deviation from cubic symmetry around the U^{+4} ion is suggested to cause the splitting of the $^3F_2'$ states. Finally, evidence for maintaining the sub-band splittings throughout the nLO sequence is also shown in figure 7(a), where clearly distinguished splittings are marked by arrows.

A level scheme is suggested in figure 8, which differs from the one presented in [1]. This scheme is consistent with the division of $\gamma_1 - \gamma_4$ into two groups of pure CF bands: γ_1, γ_3 and γ_2, γ_4 bands. According to this scheme, the ground $^3H_4'$ (Γ_5) state splits into two states (denoted as **a** and **b**) separated by ∼150 cm^{-1}. This split may be due to a Jahn–Teller effect in the paramagnetic UO_2 phase that had been previously suggested by others [24, 25].

According to the above scheme the excitations centered at 4280 (γ_2) and 4580 (γ_4) are from the lower ground state (**a**) to the $^3F_2'(\Gamma_5)$ (**c**) and $^3F_2'(\Gamma_3)$ (**d**) states, respectively. The ones centered at 4130 (γ_1) and 4420 (γ_3) are from the higher splitting of the ground state (**b**) to the **c** and **d**.

The pressure dependence of each of the four γ_1–γ_4 CF excitations is extracted from the difference between the pressure coefficients of the final and initial states. It follows that the difference between

$$\frac{\partial\omega\gamma_2}{\partial P} = \frac{\partial c}{\partial P} - \frac{\partial a}{\partial P} \qquad \text{and} \qquad \frac{\partial\omega\gamma_1}{\partial P} = \frac{\partial c}{\partial P} - \frac{\partial b}{\partial P}$$

is

$$\frac{\partial\omega(\gamma_2 - \gamma_1)}{\partial P} = \frac{\partial(b-a)}{\partial P} \approx -3\ cm^{-1}\ GPa^{-1},$$

which is practically the relative shift of the two bands under pressure. Likewise,

$$\frac{\partial\omega(\gamma_4 - \gamma_2)}{\partial P} = \frac{\partial(d-c)}{\partial P} \approx -1\ cm^{-1}\ GPa^{-1},$$

which indicates that the pressure coefficients of the two $^3F_2'$ bands seem to be comparable. Upon application of pressure

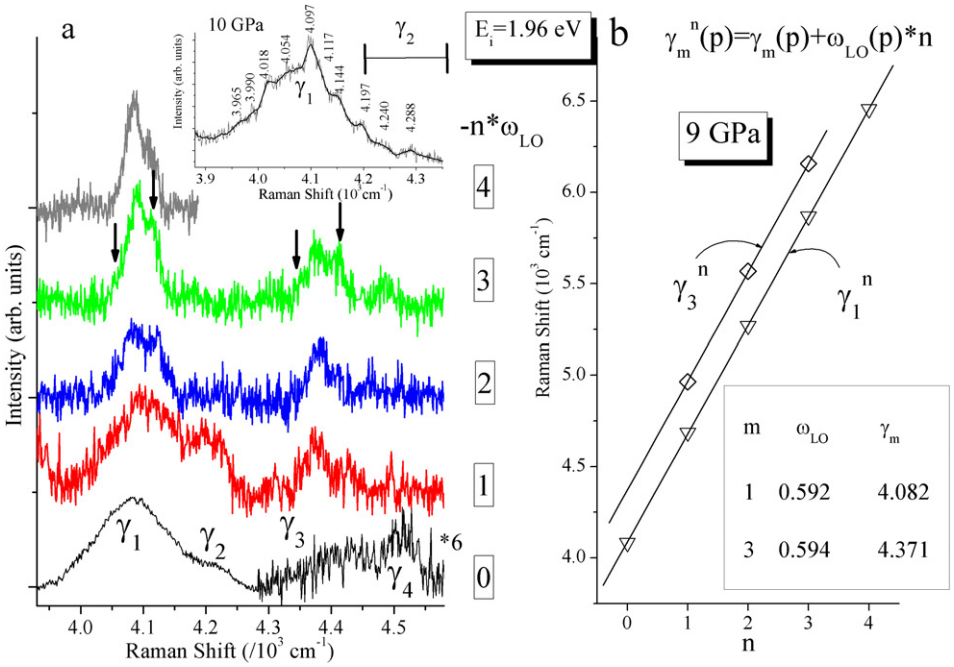

Figure 7. (a) The top spectrum from figure 6 'sliced' into segments which are shifted by $-n\omega_{\rm LO}$ (9 GPa) from their original spectral positions. In the inset the split into sub-bands of the $\gamma_1 - \gamma_2$ spectral region at 10 GPa and $E_{\rm i} = 1.96$ eV is demonstrated. Sub-band splittings, which are detected throughout the complete nLO sequence, are marked by arrows. (b) A fit to the linear equation $\gamma_m^n(P) = \gamma_m(P) + \omega_{\rm LO}(P) \cdot n$ of the central band positions for $m = 1$, 3 and $n = 0$–4.

it appears that the gap between the two $^3H'_4$ states (**a**, **b**) is reduced. It seems that the gap is not likely to disappear below the pressure where the CaF_2-type $\rightarrow$ $PbCl_2$-type structural phase transition occurs (~42 GPa) [21].

3.2.2. The $\delta(^3H'_4 \rightarrow {}^3H'_5)$ excitations. The properties of the δ and the γ bands differ in two aspects: first, the δ_1 band practically disappears around 3 GPa (with pressure coefficient $\Delta\omega\delta_1/\Delta P \approx -10$ cm^{-1} GPa^{-1} around ~2.3 GPa), while the γ_1 and is still detected around 22 GPa. Second, the tendency of the CF excitation in the Raman spectra to couple to multi-LO phonons is observed only for the latter, under ambient as well as high pressures.

It is of interest to study whether the different behavior of the γ bands and the δ band is related to the fundamentally different process that they probe. The $^3H'_4 \rightarrow {}^3F'_2$ and $^3H'_4 \rightarrow {}^3H'_5$ excitations may exhibit different sensitivity to the local environment of the U^{4+} ion. Unlike the latter $J \rightarrow J+1$ transitions, where the magnitude of the spin and angular momentum remains the same while their relative orientation (and J) is changed, in the former excitation the orbital momentum does change. For lanthanides those transitions are known to be more sensitive to the local environment around the central ion [7].

Optical reflectivity of UO_2 revealed a number of narrow optical transitions between 0.5 eV and 2 eV at pressures above ~15 GPa [13], which are attributed to transitions within the $5f^2$ multiplet of UO_2 [5–7]. The increasing strength of these normally dipole-forbidden excitations has been suggested to indicate the increasing admixture of presumably d-like character to the $5f^2$ configuration. The two bands with

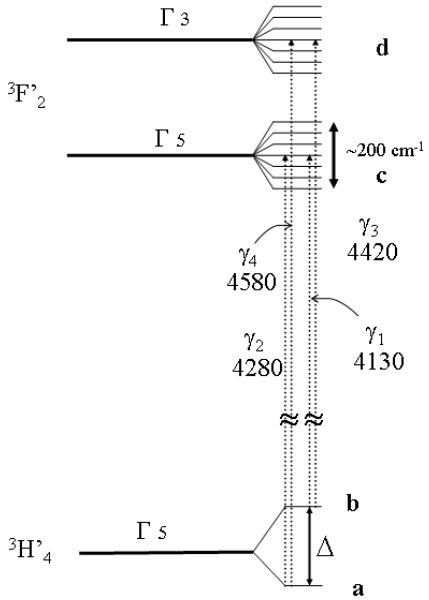

Figure 8. A suggested level scheme for the $\gamma(^3H'_4 \rightarrow {}^3F'_2)$ excitations.

lower CF transitions, with pressure coefficients $dE_{\rm CF}/dP \approx -15$ cm^{-1} GPa^{-1}, are particularly interesting. Assuming that the pressure dependence of their energies is linear, extrapolation of these bands to zero pressure is found at ~5600 cm^{-1} and ~7800 cm^{-1}, which is consistent with their assignments to $^3H'_5(\Gamma_4)$ and $^3F'_3(\Gamma_2)$ [8], respectively (see table 1). The first assignment is supported by comparable pressure coefficients of the bands found in the reflectivity [13] and in our electronic Raman spectra.

4. Conclusions

In a recent study of the phononic Raman scattering in UO_2 [10], up to sixth-order multi-LO phonon bands were detected. The Raman scattering intensity has been shown to follow the UO_2 absorption profile with threshold of ∼2.0 eV. This result has been attributed to the strong interactions between electrons and LO phonons, which play an important role in the electronic properties of UO_2. In this paper we investigate the electronic Raman scattering up to ∼1 eV and elucidate the manifestation of the strong electron–phonon interactions in the resonant coupling between nLO ($n = 1$–4) phonons and $^3H'_4 \rightarrow {}^3F'_2$ U^{4+} intermultiplet crystal-field (CF) excitations.

The resonance conditions for the CF + nLO modes are sensitive not only to excitation energy, E_i, but also to the applied hydrostatic pressure. Upon application of high hydrostatic pressure the band gap shifts to the red and the CF + nLO resonant coupling is enhanced, similar to that previously found for multi-LO phonon Raman scattering [10]. Furthermore, the pressure coefficient of the CF+nLO coupled modes frequencies fits well the sum of the pressure coefficients of their constituents.

From the four $^3H'_4 \rightarrow {}^3F'_2$ intermultiplet CF excitations which have been detected, the pairs $^3F'_2(\Gamma_5)$ and $^3F'_2(\Gamma_3)$, were expected. The additional two bands, $^3F'_2(\Gamma_5) + \Delta$ and $^3F'_2(\Gamma_3) + \Delta$ ($\Delta \approx 150$ cm^{-1}), which concurrently emerge under high pressure, are characterized by a significantly higher pressure coefficient. It is suggested that the detection of these modes is due to distortion of the lattice. The $^3H'_4(\Gamma_5)$ CF ground state splits into two states, which at ambient pressure are separated by ∼150 cm^{-1}. This separation, Δ, decreases with pressure.

Acknowledgments

I thank Dr Arye Tishbee from the Weizmann Institute of Science for allowing me to use the Renishaw dispersive Raman spectrometer. I gratefully acknowledge Dr Eran Sterer for invaluable assistance by setting up the high-pressure anvil cell.

References

[1] Schoenes J 1980 *Phys. Rep.* **63** 301
Schoenes J 1987 *J. Chem. Soc. Faraday Trans.* II **83** 1205
[2] Schaack G 2000 *Light Scattering in Solids VII* (*Springer Topics in Applied Physics* vol 75) ed M Cardona and G Güntherodt (Berlin: Springer) p 24
[3] Rahman H U and Runciman W A 1966 *J. Phys. Chem. Solids* **27** 1833
[4] Kern S, Loong C-K and Lander G H 1985 *Phys. Rev.* B **32** 3051
[5] Osborn R, Taylor A D, Bowden Z A, Hackett M A, Hayes W, Hutchings M T, Amoretti G, Caciuffo R, Blaise A and Fournier F 1988 *J. Phys. C: Solid State Phys.* **21** L931
[6] Amoretti G, Blaise A, Caciuffo R, Fournier J M, Hutchings M T, Osborn R and Taylor A D 1989 *Phys. Rev.* B **40** 1856
[7] Osborn R 1989 *Physica* B **159** 151
[8] Gajek Z, Lahalle M P, Krupa J C and Mulak J 1988 *J. Less-Common Met.* **139** 351
[9] Griffiths T R and and Hubbard H V St A 1991 *J. Nucl. Mater.* **185** 243
[10] Livneh T and Sterer E 2006 *Phys. Rev.* B **73** 085118
[11] Hyland G J 1983 *J. Nucl. Mater.* **113** 125
Cassado J M, Harding J M and Hyland G J 1994 *J. Phys. Condens. Matter* **6** 4685
[12] Ruello P, Becker R D, Ullrich K, Desgranges L, Petot C and Petot-Ervas G 2004 *J. Nucl. Mater.* **328** 46
[13] Syassen K, Winzen H and Benedict U 1986 *Physica* B **144** 91
Benedict U, Andreetti G D, Fournier J M and Waintal A 1982 *J. Physique* **43** L-171
Benedict U 1994 *J. Alloys Compounds* **213/214** 153
[14] Sterer E, Pasternak M P and Tailor R D 1991 *Rev. Sci. Instrum.* **63** 1117
[15] Mao H K, Xu J and Bell P M 1986 *J. Geophys. Res.* **91B** 4673
[16] Heyen E T, Wegerer R, Schönherr E and Cardona M 1999 *Phys. Rev.* B **44** 10195
[17] Güntherodt G, Gayaraman A, Batlogg G, Croft M and Melczer E 1983 *Phys. Rev. Lett.* **51** 2330
[18] Loewenhaupt M and Witte U 2003 *J. Phys.: Condens. Matter* **15** S519
[19] Thalmeier P and Flude P 1982 *Phys. Rev. Lett.* **49** 1588
[20] Guncharov A F, Struzhkin V V, Ruf T and Syassen K 1994 *Phys. Rev.* B **50** 13841
[21] Idri M, Le Bihan L T, Heathman S and Rabizant J 2004 *Phys. Rev.* B **70** 014113
[22] Gregorian T, d'Amour-Sturm H and Holzapfel W B 1989 *Phys. Rev.* B **39** 12497
[23] Jayasankar C K, Ramanjaneya Setty K, Babu P, Tröster Th and Holzapfel W B 2004 *Phys. Rev.* B **69** 214108
[24] Caciuffo R, Amoretti G, Santini P, Lander G H, Kulda J and Du Plessis P de V 1999 *Phys. Rev.* B **59** 13892
[25] Sasaki K and Obata Y 1970 *J. Phys. Soc. Japan* **28** 1157